Available online at www.sciencedirect.com

SCIENCE DIRECT®

ELSEVIER

Dyes and Pigments 61 (2004) 31–38

DYES and PIGMENTS

www.elsevier.com/locate/dyepig

Preparation of nanometer-sized (1−x) $SnO_2 \cdot xSb_2O_3$ conductive pigment powders and the hydrolysis behavior of urea

Junru Tan*, Lazhen Shen, Xiansong Fu, Wenxiang Hou, Xiuzeng Chen

Department of Chemistry, College of Science, Tianjin University, Tianjin, 300072, PR China

Received 1 June 2003; received in revised form 16 June 2003; accepted 4 August 2003

Abstract

Nanometer-sized spherical (1−x) $SnO_2 \cdot xSb_2O_3$ conductive pigment powders, with a resistivity of 36.70 Ω·cm and particle size of about 10 nm, have been prepared by using homogenous precipitation method with urea as precipitant. This paper discussed the effects of the molar ratio of Sn^{4+}/Sb^{3+} and the reaction system temperature on the electrical conductivity of the pigment. The relation between calcining temperature and particle morphology, particle size, specific surface area and resistivity were described. Finally, the hydrolysis reaction kinetics of urea and the reaction activation energy obtained by calculating the hydrolysis reaction kinetics of urea were discussed.

Keywords: Conductive pigment; (1−x) $SnO_2 \cdot xSb_2O_3$; Homogenous precipitation method; Urea; Calcine; Reaction kinetics

1. Introduction

Polymeric materials are used widely for industry and everyday life because they are good insulators and easy to be processed. But the friction or impaction on polymeric materials surface can easily lead to static aggregation due to their high insulating property. Since the electrostatic accumulated on the surface is difficult to purify, it will influence appearance and application of the product in super clean circumstances. A more serious problem is that when electrostatic is accumulated to certain degree, it will let out electricity and cause precision instruments or precision electronics to be broken down and be scrapped. Therefore, the electrostatic dangers get more attention [1]. When added to the surface of the coating and coated product, a conductive pigment can cause conductivity, anti-static and shielding to electromagnetic waves, etc. [2]. Thus, a diverse range of applications have been found, such as in mining, oil–gas field, the chemical industry, automobiles and the aerospace industry and for packing materials of integrated circuits and electronics. It is a conductive material with excellent development potentiality [3]. Conductive pigments consist of a carbon series conductive pigment, a metallic conductive pigment and a metal oxide conductive pigment, based on the difference of materials. Among them, a carbon series conductive pigment has good conductive properties, while it is dull and dark in color and has poor adhesive force and resistance to oil [4]. A metallic conductive pigment

---

* Corresponding author.
E-mail address: tjunru@yahoo.com (J. Tan).

0143-7208/$ - see front matter © 2003 Elsevier Ltd. All rights reserved.
doi:10.1016/j.dyepig.2003.08.005

has a large specific gravity and the surface is easy to be oxidized, and because of its high cost, industry production is limited. Thus, the development of a composite conductive pigment is very active, and now there are many patents reported for this [5,6]. The main system is semi-conductive powder doped with another element or compound by using SnO_2 as a precursor. There are many methods reported for the preparation of conductive pigment powders, e.g. dry method [7] and wet method. Wet methods include a alkoxide hydrolysis method, sol-gel method [8] and a co-precipitation method [9], etc. In the present study, an attempt has been made to prepare nanometer-sized spherical $(1-x)\ SnO_2{\cdot}xSb_2O_3$ conductive pigment powder (ATO) by using a homogenous precipitation method with urea as the precipitant. The resistivity of the pigment is 36.70 Ω·cm and the particle size is around 10 nm. This paper studies the preparation method of ATO, the effects of main technological parameters on its properties, the hydrolysis behavior of the precipitant in the reaction process and the calculation of the reaction activation energy.

2. Experimental

2.1. Materials

Tin tetrachloride: $SnCl_4{\cdot}5H_2O$ (analytical reagent), antimony butter: $SbCl_3$ (analytical reagent) and sodium hydroxide: NaOH (chemical reagent) were used as starting chemicals. Precursor solutions of $SnCl_4{\cdot}5H_2O$ (1.0 M), $SbCl_3$ (0.1 M) and NaOH (2.0 M) were prepared in distilled water. Urea: $CO(NH_2)_2$ (analytical reagent) was used as the precipitant and *p*-dimethylaminobenzaldehyde (analytical reagent) was used as an indicator of urea.

2.2. Property characteristics

The resistivity was calculated as follows: firstly, ATO powders were pressed to a circular flat chip of 12 mm diameter under 2.5 ton pressure by using a MYI-50 sheeter, then put this chip between two sheets of copper. Its volume resistance was measured by using a multimeter and its thickness was obtained by vernier caliper. The resistivity was calculated by using the formula $\rho = R \cdot \frac{A}{d}$, where ρ is resistivity, R is actual resistance, A is the cross section area of chip, and d is the chip's thickness. Scanning electron microscopy (SEM JEDL100CX II) was used to estimate particle morphology, nature of agglomerates and particle size in the resultant pigment powders. The absorbance of the reaction system was obtained by using a spectrophotometer (721) to study the hydrolysis of urea. The phase analysis of Sb_2O_3 at different calcining temperatures was carried out by X-ray diffractometer (XRD BDX-3300).

2.3. Preparation method of ATO

A mixture of $SnCl_4$ solution and $SbCl_3$ solution was treated in a 250 ml reaction vessel with the molar ratio of $Sn^{4+}/Sb^{3+} = 12.5{:}1$, followed by adding some urea and deionized water with continuous stirring. This mixing solution was heated to 368 K to react. When the pH value of the reaction system reached 5.0–6.0, we took a reactant to centrifugalize, then added 2.0 mol L^{-1} NaOH solution in supernatant, if there was no precipitate appearing, we can judge that the reaction is finished. The temperature was maintained for 1 h with continuous stirring. The resultant powders were washed with distilled water several times until there was no Cl^- ion in the resultant powders and then filtered. Finally, the resultant powders were dried at 353 K and the ATO precursor obtained, then were calcined in 973 K for 0.5 h and obtained ATO (Antimony Doped Tin Dioxide) pigment with excellent conductivity and about 10 nm of particle size. The reaction processes are:

$$CO(NH_2) + 3H_2O \leftrightarrows NH_3 \cdot H_2O + CO_2 \quad (1)$$

$$NH_3 \cdot H_2O \leftrightarrows NH_4^+ + OH^- \quad (2)$$

$$Sn^{4+} + 4OH^- \rightarrow Sn(OH)_4 \xrightarrow{\Delta} SnO_2 + 2H_2O \quad (3)$$

$$2Sb^{3+} + 6OH^- \rightarrow 2Sb(OH)_3 \xrightarrow{\Delta} Sb_2O_3 + 3H_2O \qquad (4)$$

3. Conclusion and discussion

3.1. Optimum molar ratio of Sn^{4+} to Sb^{3+}

The content of antimony in ATO pigment influences the pigment's electrical conductivity directly. With other experimental conditions fixed, we changed the molar ratio of Sn^{4+}/Sb^{3+} and measured the resistivity of the pigment powders. The results are shown in Fig. 1.

Fig. 1 describes that the resistivity decreases and the electrical conductivity increases with the molar ratio of Sn^{4+}/Sb^{3+} decreasing at the beginning, and the electrical conductivity of ATO is best at molar ratio = 12.5:1 (mean 100:8). But with the molar ratio of Sn^{4+}/Sb^{3+} continuously decreasing, the resistivity increases and the electrical conductivity becomes poor. The reason is that when the molar ratio of Sn^{4+} to Sb^{3+} is high, a small amount of Sb causes a crystal defect to form a conductive current carrier to have electrical conductive, and the concentration of current carrier increases and the electrical conductivity becomes better with Sb content increasing. But when the molar ratio of Sn^{4+}/Sb^{3+} is low, that is, the doping quantity is too much, although the concentration of conductive current carrier increases, the concentration of ionization impurity also increases at the same time, which increases the scattering action to current carrier and decreases directional drift moving of the current carrier, further decreases the mobility ratio of the current carrier to make the electrical conductivity decrease. Thus the optimum molar ratio of Sn^{4+} to Sb^{3+} is 100:8 (mean 12.5).

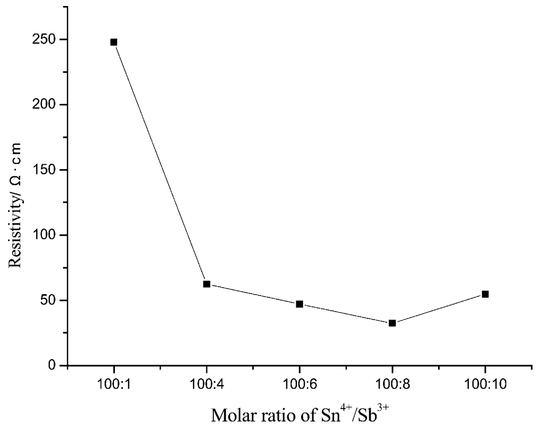

Fig. 1. Relation of molar ratio of Sn^{4+}/Sb^{3+} and resistivity of ATO.

3.2. Reaction temperature

The reaction temperature is very important by using urea as precipitant because the concentration of the OH^- ion is directly controlled by the hydrolysis rate of urea. When the reaction temperature is low, urea hydrolyzes very slowly and the reaction time is too long, while very high temperature can lead to fast hydrolysis of urea, very large supersaturating degree in the reaction system and a high nucleation rate, but causes the crystal nucleus to grow slowly. Thus the particles obtained are very tiny and become a colloidal dispersion and they are very difficult to filter and wash. With other experimental conditions fixed, the resistivities of the samples by varying temperature were measured and shown in Table 1.

From Table 1, we can see that with temperature increasing, the reaction time reduces and the resistivity decreases, however, the resistivity increases at a certain temperature. The resistivity of the sample is the smallest and the electrical conductivity is the best at 363 K and under these conditions, most likely due to the reaction system being in the optimum supersaturating state and

Table 1
Reaction time and resistivities of ATO at different temperatures

Reaction temperature (K)	Reaction time (h)	Resistivity (Ω·cm)
353	54	165.11
358	18	46.40
363	13	21.94
368	6	36.70

microcosmic mixing state. Finally by considering both reaction time and electrical conductivity, we choose 368 K as the reaction temperature.

3.3. Calcining temperature

3.3.1. Relation of calcining temperature and electrical conductivity

ATO precursors were prepared under optimum conditions and were calcined at 673, 773, 873, 973, 1073, 1173 and 1273 K respectively. The results of the resistivities of the samples measured are shown in Fig. 2.

Fig. 2 shows that the electrical conductivity is poor at 673 K. The reason is that Sb^{3+} ions enter into SnO_2 crystal and further replace Sn^{4+} lattice sites, which can be explained by the fact that there are only Sb_2O_3 diffraction peaks at 673 K in the XRD patterns of Sb_2O_3 (Fig. 3). The defect formed by Sb^{3+} ion replacing Sn^{4+} lattice site is equal to binding a vacancy flabbily around a negative. The localized energy level of the defect located near the top of valence band, and the vacancy bound flabbily is excited to fall in the valence band by attaining certain energy to have electronic conductivity and thermal conductivity. Thus SnO_2 crystal forms a P-type semiconductor. This is likely to be caused by the relatively difficult replacement because the radius of Sb^{3+} ion is slightly larger than that of Sn^{4+} ion and the calcining temperature of 673 K is low. The less current carrier formed led to a poor electrical conductivity. The electrical conductivity of ATO increases with calcining temperature increasing between 673 and 1073 K. The reason maybe is that Sb^{3+} ions are oxidized to Sb^{5+} ions gradually and the radius of Sb^{5+} ion is smaller than that of Sn^{4+} ion to replace Sn^{4+} lattice site easily. The defect formed by the replacement of Sn^{4+} lattice site with the Sb^{5+} ion is equal to a monovalent cation bound flabbily by an electron (Sb^{+}_{Sn}). The defect can give out electron with the formula of $Sb^{\times}_{Sn} + E_D \rightarrow Sb^{\cdot}_{Sn} + e'$ to show as a donor defect and form an N-type semiconductor. When the energy of defect accepted is larger than or equal to E_D, the electron can be excited into conduction band to form a conductive current carrier. Because the mobility rate of the electron is larger than that of the cavity [10], the result shows an increase in electrical conductivity as shown in Fig. 2. While with calcining temperature increasing above 1073 K, the resistivity of ATO increases and the electrical conductivity decreases. The reason maybe is that Sb^{5+} ions are reduced to Sb^{3+} ions partly, leading to a decrease of Sb^{5+} ions to replace Sn^{4+} lattice sites and a decrease of electron current carrier, but an increase of cavity current carrier. The XRD patterns of the single Sb_2O_3 at different calcining temperatures match very well with this as shown in Fig. 3.

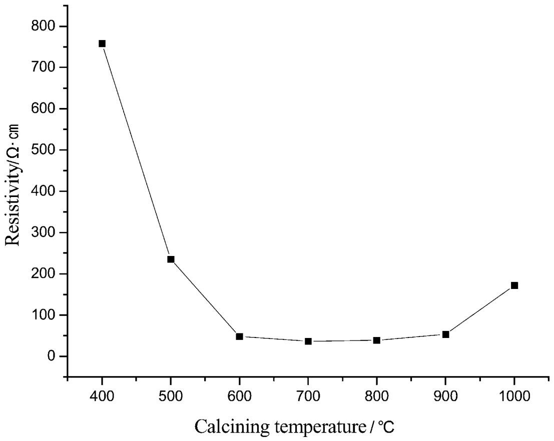

Fig. 2. Electrical conductivities at different calcining temperatures.

From Fig. 3, we can see that there is no Sb_2O_4 (compound of Sb_2O_3 and Sb_2O_5) diffraction peak when calcined at 673 K [Fig. 3(1)]. The absence of 2θ angles of 29.00, 30.30, 33.72, 37.34 and 48.82° indicates that the diffraction peaks of Sb_2O_4 are present in XRD patterns of 773–1173 K and illustrate the appearance of Sb_2O_5. While the strength of peaks (e.g. 2θ of 30.30°) become weakened at 1173 K again, which illustrates the change of oxidation state of antimony.

3.3.2. Relation of the calcining temperature and specific surface area

ATO precursor prepared under optimum conditions was calcined at 873, 973 and 1073 K for the same time respectively to get ATO pigment powders. The resistivities of ATO pigment powders were measured and given in Table 2.

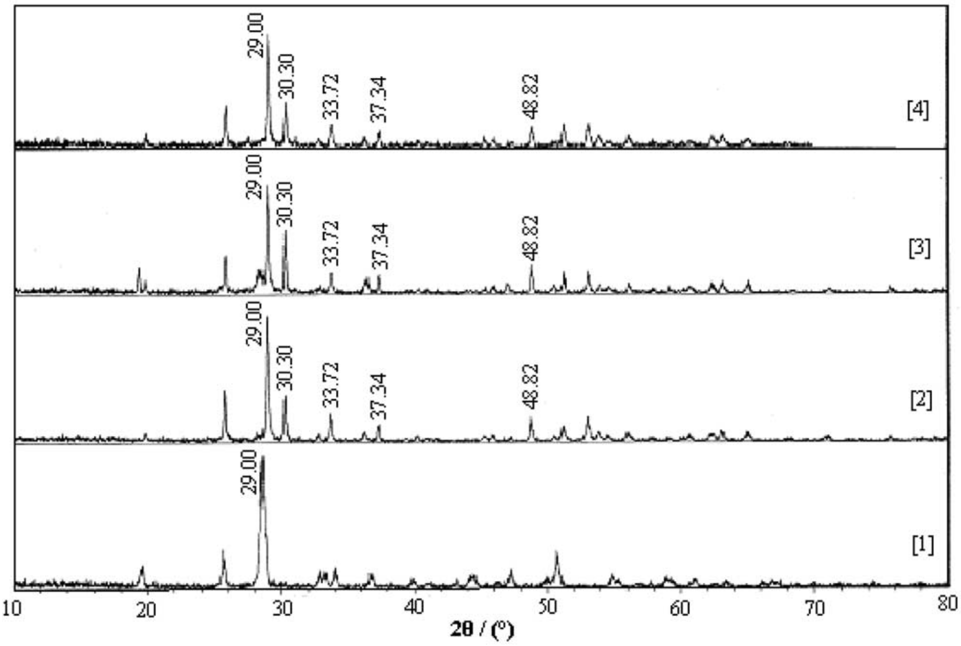

Fig. 3. X-ray diffraction patterns of Sb_2O_3 of different calcining temperatures (1) 673 K, (2) 773 K, (3) 973 K, (4) 1173 K.

The relative TEM micrographs of ATO powders at different calcining temperatures are shown in Fig. 4.

Based on data of Table 2, the specific surface area of ATO decreases with the calcining temperature increasing to indicate that the particle size of ATO powders becomes larger. The TEM micrographs of ATO powders (Fig. 4) show that the particle size of ATO powders increases with the calcining temperature, which agrees very well with the data as given in Table 2. The reason for the decrease of specific surface area of ATO powders is that in the process of calcining, substances diffuse on the microcrystallite surface and inside microcrystallite mainly by surface diffusion. The reaction driving force is due to the decrease of free surface energy of particles [11]. For two particles contacting each other both having large surface energy, the substances inside them move and the surface energy decreases when heated to below their melting point to make the two particles melt together and the particle size increase, which leads to a decrease of specific surface area.

Table 2
Specific surface areas at different calcining temperatures

Calcining temperature (K)	Specific surface area (m^2 g^{-1})
Not calcining	67.08
600	48.34
700	46.43
800	34.58

3.4. Hydrolysis kinetics of urea

The concentration of urea decreases gradually with the reaction going on, so there is a color difference when urea reacts with urea indicator *p*-dimethylaminobenzaldehyde. The absorbance of different concentration of urea was obtained by using a spectrophotometer (721) to calculate the concentration of urea at a certain reaction time.

3.4.1. Determination of working curve of urea

A spectrophotometer (721) was used to obtain the absorbance of different concentration of urea with same volume by adding same quantity of urea indicator with distilled water as reference sample. A plot of the concentration of urea

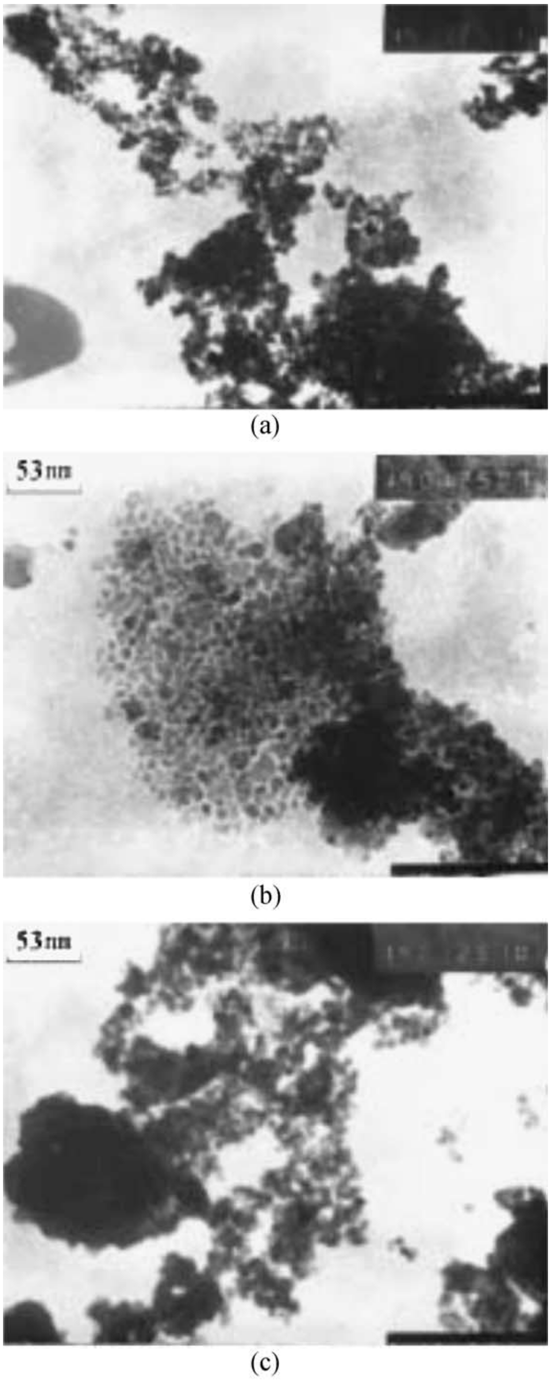

Fig. 4. The TEM micrographs of ATO powders (a) 873 K, (b) 973 K, (c) 1073 K.

against absorbance was given out by using urea concentration (C) as ordinate and absorbance (A) as abscissa as shown in Fig. 5.

The concentration of urea is linear with absorbance and the linear equation is given as the following equation:

$$C = 0.08228A - 0.00277$$

The concentration of urea at a given time can be calculated from this equation by measuring the absorbance at this moment.

3.4.2. Reaction rate equation of urea hydrolysis

The whole reaction consists of several steps to prepare the co-precipitate of $Sn(OH)_4$ and $Sb(OH)_3$ by the hydrolysis of urea. Among these steps, the reaction of urea hydrolysis is the slowest step, which should be the control step of rate. That is, the whole reaction rate can be approximately equal to the reaction rate of urea hydrolysis. So we can assume that the whole reaction acts as the simplest first order reaction [12] shown as the following:

$$v = kC \tag{5}$$

$$v = -\frac{dC}{dt} = kC \tag{6}$$

$$-\frac{dC}{C} = k dt, \tag{7}$$

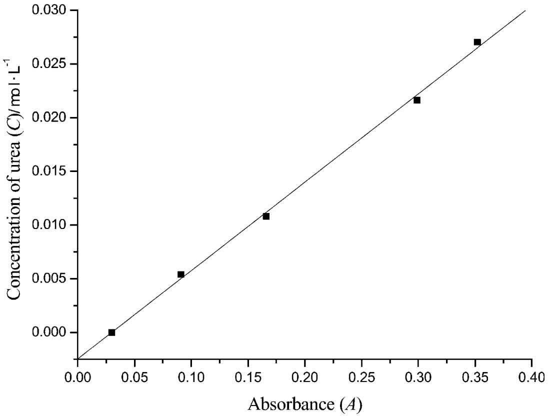

Fig. 5. Plot of concentration of urea against absorbance.

where v is the reaction rate of hydrolysis, k is the rate constant, C is the concentration of urea, and t is the reaction time.

A sample taken out once half an hour was cooled down quickly and further was centrifuged. Supernatant liquid (0.2 ml) of the sample obtained by centrifugal separation was pumped off by a micro injector and treated in a 50 ml volumetric flask, followed by adding several drops of urea indicator, and was diluted with distilled water to scale mark of volumetric flask to be a uniform solution. Absorbance of the sample was obtained from this solution by using a spectrophotometer. The concentration of urea was calculated according to the absorbance of sample. For example, the absorbance and the concentration of urea at different reaction time with the reaction temperature being 368 K are given in Table 3.

Eq. (7) was integrated and got a formula as following:

$$-\ln C = kt + B \tag{8}$$

where B is a constant. To make a chart of $-\ln C$ versus t, a straight line can be obtained as shown in Fig. 6.

The slope of this line is just the rate constant k. The equation of this line is $-\ln C = 0.110t + 4.648$, and the rate constant $k_1 = 0.110\text{h}^{-1}$ at 368 K can be obtained by this equation. Using the same method, the rate equation and rate constant of 373 and 378 K are all obtained and given as following:

$$-\ln C = 0.137t + 4.036, \quad k_{2(373\text{K})} = 0.137\,\text{h}^{-1}$$

$$-\ln C = 0.181t + 4.116, \quad k_{3(378\text{K})} = 0.181\,\text{h}^{-1}$$

Table 3
Absorbance and concentration of urea at 368 K

Time (h)	Absorbance	Concentration of urea (mol L^{-1})	$-\ln C$
0.5	0.209	0.0147	4.218
1.0	0.198	0.0138	4.282
1.5	0.190	0.0132	4.330
2.0	0.182	0.0125	4.382
2.5	0.176	0.0120	4.422
3.0	0.164	0.0110	4.508

3.4.3. Calculation of activation energy of urea hydrolysis during ATO preparation

The equation shown as following

$$\ln k = -\frac{E_a}{RT} + \ln A \tag{9}$$

is obtained based on the Arrhenius equation:

$$k = A e^{-\frac{E_a}{RT}} \tag{10}$$

where E_a is the Arrhenius activation energy, R is the gas constant, T is the thermodynamic temperature, and A is a constant. A straight line can be got by making a chart of $\ln k$ versus T^{-1}, and its slope is $\alpha = -\frac{E_a}{R}$, that is,

$$E_a = -\alpha R \tag{11}$$

The activation energy can be calculated by Eq. (11). The $\ln k$ at different temperatures are linear with T^{-1} as shown in Fig. 7.

An equation can be obtained and shown as following by Fig. 7:

$$\ln k = -6.984/T + 16.749 \tag{12}$$

the slope is $\alpha = -6.984 = -\frac{E_a}{R}$, so we can get the value of activation energy E_a: $E_a = \alpha R = 6.984 \times 8.314 = 58.064$ (kJ mol^{-1})

Therefore, the activation energy of urea hydrolysis in the reaction system is 58.064 kJ mol^{-1} l^{-1}.

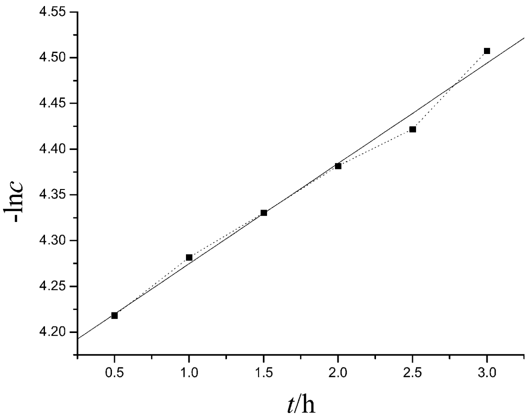

Fig. 6. Chart of $-\ln C$ versus t at 368 K.

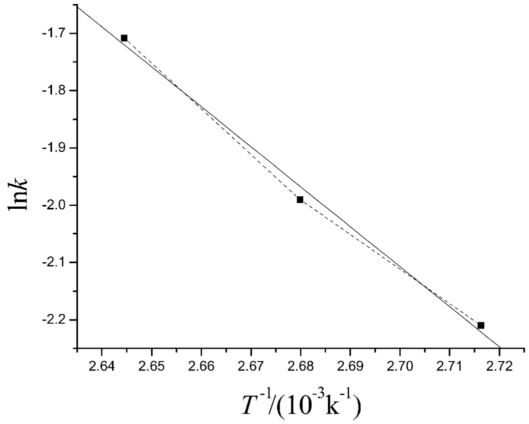

Fig. 7. Linear relation of ln*k* and T^{-1}.

4. Conclusion

An homogenous precipitation method with urea as the precipitant is successfully used to prepare nanometer-sized (about 10 nm) spherical $(1-x)$ $SnO_2 \cdot xSb_2O_3$ conductive pigment powders with a resistivity of 36.70 Ω·cm. The optimum technological parameters are shown below: the molar ratio of Sn^{4+} to Sb^{3+} is 12.5:1 and the reaction system temperature is 368 K. With calcining temperature increasing, ATO particle size increases but specific surface area decreases, the resistivity decreases at first while increasing later, most likely due to the change of oxidation number of Sb. The step of urea hydrolysis is the control step in the whole reaction process and the activation energy of urea hydrolysis is 58.064 kJ mol^{-1} l^{-1}.

References

[1] Liu GB, Liang GM, Xu H. A light-coloring conductive dyestuff. Journal of Chongqing Normal University 1998; 15(1):33–6.

[2] Xia H, Zhang W, Qian JR. Preparation of white electrically conductive pigment. Fine Chemicals 2000;17(5): 284–6.

[3] Kaneko K, Sakurai H, Izumi K. Heat-ray shading film. [P] JP: 10-100310,1998.

[4] Sun JT. Application of composite conductive mica powder to preventing electrostatic pigment. Shanghai Coatings 1999;(4):31–3.

[5] Bruckner Hans-Dieter DR. Electrically conductive pigmentary platelets. [P] DE3842330, 1990-06-20.

[6] Wright FA. Metal-coated hollow microspheres. [P] US4621024, 1986-11-04.

[7] Bo ZM, Xu X, Qu YF. Investigation on conducting ceramics. Bulletin of the Chinese Ceramic Society 1992;(5):15–17.

[8] Pan QY, Xu JQ, Dong XW. Preparation of nanometer-sized SnO_2 and its gas sensitive properties. Journal of East China University of Science and Technology 1998;24(4): 431–5.

[9] Li BS, Zhang JC, Song B. Influences of heat-treatment on the particle size and properties of conductive nanometer-sized antimony-doped tin dioxide powders. Journal of Inorganic Materials 2002;17(3):489–96.

[10] Liu EK, Zhu BS, Luo JS. Semiconductor physics. Beijing: National Defence Industry Publication; 1994;84–93:96–100.

[11] Zhu YH, Li CZ, Hu LM, et al. Mechanism of micropore disappearing in the later period of α-FeOOH dehydration. Journal of East China University of Science and Technology 1995;21(5):567–8.

[12] Wuhan University. Inorganic chemistry. Beijing: Higher Education Publication; 1995. p. 287.